Behaviors of Anisotropic Fluids in the Vicinity of a Wedge

Youn J. Kim*
School of Mechanical Engineering, Sungkyunkwan University

The laminar boundary layer flow and heat transfer of anisotropic fluids in the vicinity of a wedge have been examined with constant surface temperature. The similarity variables found by Falkner and Skan are employed to reduce the streamwise-dependence in the coupled nonlinear boundary layer equations. The numerical solutions are presented using the fourth-order Runge-Kutta method and the distribution of velocity, micro-rotation, shear and couple stresses and temperature across the boundary layer are plotted. These results are also compared with the corresponding flow problems for Newtonian fluid over wedges. It is found that for a constant wedge angle, the skin friction coefficient is lower for micropolar fluid, as compared to Newtonian fluid. For the case of the constant material parameter K, however, the magnitude of velocity for anisotropic fluid is greater than that of Newtonian fluid. The numerical results also show that for a constant wedge angle with a given Prandtl number, $Pr=1$, the effect of increasing values of K results in increasing thermal boundary layer thickness for anisotropic fluid, as compared with Newtonian fluid. For the case of the constant material parameter K, however, the heat transfer rate for anisotropic fluid is lower than that of Newtonian fluid.

Key Words : Anisotropic Fluids, Similarity, Wedge, Micro-Rotation

Nomenclature

C_f : Local skin friction coefficient
f : Reduced stream function
h : Dimensionless microrotation
h_t : Heat transfer coefficient
j : Micro-inertia density
K : Dimensionless parameter of vortex viscosity
m : Falkner-Skan power-law parameter
Re : Reynolds number
T : Temperature
u, v : Fluid velocities in the x and y directions, respectively
U : Free stream velocity
x : Streamwise coordinate along the body surface
y : Coordinate normal to the body surface

Greek symbols

α : Thermal diffusivity
β : Wedge angle parameter
γ : Spin gradient viscosity
η : Pseudo-similarity variable
$\varkappa$: Vortex viscosity
μ : Absolute viscosity of the fluid
ν : Kinematic viscosity
ρ : Density of micropolar fluid
τ : Shear stress
ω : Angular velocity of micropolar fluid
ξ : Coefficient of viscosity
ψ : Stream function
ζ : Coefficient of viscosity
θ : Dimensionless temperature

* **E-mail** : kimyj@me.skku.ac.kr
TEL : +82-331-290-7448 ; **FAX** : +82-331-295-1937
School of Mechanical Engineering, Sungkyunkwan University 300 Chunchun-dong, Suwon 440-746, Korea. (Manuscript **Received** March 25, 1999; **Revised** March 7, 2000)

1. Introduction

At present there exist several approaches to the formulation of fluids that contain structures, and these fluids are called by various names such as - simple microfluids, micropolar fluids, deformable directed fluids, polar fluids, anisotropic fluids,

etc.

The theory of micropolar fluids which display the microscopic effects arising from the local structure and micro-motions of the fluid elements, was formulated by Eringen (1966, 1972). This is a recent development in continuum mechanics, and has attracted the attention of several investigators (Bergholz, 1980; Emra and Kulacki, 1980; Chandra Shekar *et al.*, 1984) because of their industrial applications. Experiments with fluids containing extremely small amount of polymeric additives indicate that the skin friction near a rigid body in such fluids are considered lower (up to 30-35%) than the same fluids without additives. The classical Navier-Stokes theory is incapable of predicting these findings since it contains no mechanism to explain this new physical phenomenon.

Physically, the mathematical model underlying the anisotropic fluids may represent the behavior of polymeric additives, blood, lubricants, liquid crystals, dirty oils and colloidal suspension solutions. The theory of such fluids has been attracted considerable attention. For example, with the aid of Karman-Polhausen integral method, Willson (1970) obtained the approximate solution of boundary layer micropolar fluids flow over a semi-infinite flat plate. Ahmadi (1976) has provided a similarity solution for the micropolar boundary layer flow over a semi-infinite flat plate. Ariman (1971) applied the micropolar fluid theory to the analysis of blood flow for small arteries of the order of 100μm diameter. He compared the velocity profiles with the existing experimental data under the assumption of zero micro-rotation at the walls and showed a good agreement.

Rees and Bassom (1996) have studied the micropolar analogue of the Blasius boundary layer flow. They derived non-similar boundary layer equations and solved using the Keller-box method. They also performed an asymptotic analysis for large distances from the leading edge because the numerical results indicatd that the boundary layer developed as a two-layer structure.

Gorla (1980) applied the micropolar boundary layer theory to the problem of two-dimensional steady stagnation point flow with constant wall temperature. He mentioned that the numerical results could use for drag reduction purposes or heat transfer rate augmentation in heat exchangers. Gorla (1984, 1985) also investigated the boundary layer characteristics of an axisymmetric, laminar, micropolar fluid flow with a uniform velocity U along a horizontal cylinder. He presented the numerical solutions for the velocity, micro-rotation and heat transfer fields for a wide range of values of the dimensionless curvature parameter as well as material parameters.

The purpose of this paper is to introduce a general transformation procedure appropriate to the problem of boundary layer flow of an anisotropic fluid in the vicinity of a wedge. It is necessary to consider in detail the distribution of velocity and temperature distributions across the boundary layer, in addition to the surface skin friction. The problem under study is modelled as a boundary value problem by introducing a similarity transformation and numerical solutions are presented.

2. Mathematical Formulation

Eringen (1966) derived the following constitutive equations for anisotropic fluids that giving the viscous stress τ_{ij}, and the couple stress tensor m_{ij} in Cartesian tensor notation, as follows:

$$\tau_{ij}=(-p+\lambda v_{r,r})\,\delta_{ij}+\mu(v_{i,j}+v_{j,i}) +\chi(v_{j,i}-\varepsilon_{ijr}\omega_r) \tag{1}$$

$$m_{ij}=\zeta\omega_{r,r}\delta_{ij}+\xi\omega_{i,j}+\gamma\omega_{j,i} \tag{2}$$

where p is the pressure, δ_{ij} is the Kronecker symbol, ε_{ijr} is an alternating tensor and the summation convention has been used. Furthermore, $v_{i,j}$ is the velocity gradient tensor, ω_r the micro-rotation velocity vector, μ the coefficient of viscosity, χ the coefficient of gyro-viscosity (or vortex viscosity) and λ, ξ and ζ are material constants.

Consider a two-dimensional steady flow of laminar, incompressible, anisotropic fluid flow in

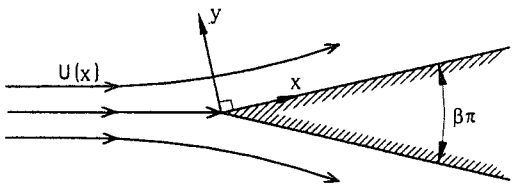

Fig. 1 The physical model and coordinate system

the vicinity of a wedge with constant wall temperature. The physical model and geometrical coordinates are shown in Fig. 1. Let u, v be the velocities along and perpendicular to the body surface, all being functions of x and y. The effects of viscous dissipation will be assumed to be negligible. Under the usual boundary layer approximation, the governing conservation equations for the steady, laminar, incompressible, anisotropic fluid flow in the vicinity of a wedge can be casted into the nondimensional form with the absence of body forces and body couples, as follows (Ahmadi, 1976):

mass:

$$\frac{\partial u}{\partial x}+\frac{\partial v}{\partial y}=0 \tag{3}$$

momentum:

$$\rho\left(u\frac{\partial u}{\partial x}+v\frac{\partial u}{\partial y}\right)=-\frac{\partial p}{\partial x}+(\mu+\chi)\frac{\partial^2 u}{\partial y^2}+\chi\frac{\partial \omega}{\partial y} \tag{4}$$

angular momentum:

$$\rho j\left(u\frac{\partial \omega}{\partial x}+v\frac{\partial \omega}{\partial y}\right)=\frac{\partial}{\partial y}\left(\gamma\frac{\partial \omega}{\partial y}\right)-\chi\left(2\omega+\frac{\partial u}{\partial y}\right) \tag{5}$$

micro-inertia:

$$u\frac{\partial j}{\partial x}+v\frac{\partial j}{\partial y}=0 \tag{6}$$

energy:

$$u\frac{\partial T}{\partial x}+v\frac{\partial T}{\partial y}=\alpha\frac{\partial^2 T}{\partial y^2} \tag{7}$$

where ρ is the density, j the micro-inertia density, T the fluid temperature, α the thermal diffusivity, and ω the component of micro-rotation vector normal to the xy-plane.

Furthermore, the spin-gradient viscosity γ, which gives some relationship between the coefficients of viscosity and micro-inertia, is defined as

$$\gamma=\left(\mu+\frac{\chi}{2}\right)j \tag{8}$$

The above governing equations need to be solved subject to the following boundary conditions on velocity, micro-rotation and temperature fields:

$$u=0,\ v=0,\ w=-\frac{1}{2}\frac{\partial u}{\partial y},\ T\rightarrow T_w \quad \text{on } y=0 \tag{9}$$

$$u\rightarrow U,\ v\rightarrow 0,\ \omega\rightarrow 0,\ T\rightarrow T_\infty \quad \text{as } y\rightarrow\infty \tag{10}$$

where U the free stream velocity. The boundary condition (9) represents weak concentrations and means that the micro-rotation is equal to a half of the fluid vorticity at the boundary.

The most famous family of boundary-layer similarity solutions was formulated by Falkner and Skan (1930). They found that similarity was achieved by the variable $\eta=yg(x)$, which was consistent with a power-law free stream velocity distribution:

$$U(x)=Cx^m \tag{11}$$

where the exponent m be termed the Falkner-Skan power-law parameter, and is related to the wedge angle $\beta\pi$ by

$$\beta=\frac{2m}{1+m} \tag{12}$$

When β is positive, the free-stream velocity increases along the wedge surface; for negative β, it decreases.

In this study we adopted their techniques, and introduced the following transformations:

$$y=\left[\frac{2\nu x}{(m+1)\,U(x)}\right]^{1/2}\eta=\frac{1}{g(x)}\eta,$$

$$\psi=\left[\frac{2\nu x U(x)}{(m+1)}\right]^{1/2}f(\eta)$$

$$\omega=U(x)\left[\frac{(m+1)\,U(x)}{2\nu x}\right]^{1/2}h(\eta),$$

$$j=\frac{2\nu x}{(m+1)\,U(x)}i,$$

$$\gamma=\left[\mu+\frac{\chi}{2}\right]\frac{2\nu x}{(m+1)\,U(x)}i,$$

$$u=U(x)f',$$

$$v=-\left[\frac{\nu U(x)}{2(m+1)x}\right]^{1/2}\{(m+1)f+\eta(m-1)f'\},$$

$$\theta=\frac{T-T_\infty}{T_w-T_\infty} \tag{13}$$

where a prime represents differentiation with respect to η. The continuity equation is automatically satisfied by a stream function ψ such that:

$$u=\frac{\partial\psi}{\partial y},\ v=-\frac{\partial\psi}{\partial x} \tag{14}$$

With the aid of the above transformations, the boundary layer Eqs. (4)-(7) can be written as

$$(1+K)f^m+Kh'+ff''+\frac{2m}{m+1}[1-(f')^2]=0 \tag{15}$$

$$\left[1+\frac{K}{2}\right](ih')'-K(2h+f'')=i\left[\left[\frac{3m-1}{m+1}\right]f'h-fh'-\left[\frac{m}{m+1}\right]\eta f'h'\right] \tag{16}$$

$$\frac{2(m-1)}{m+1}f'i+fi'=0 \tag{17}$$

$$\theta''+f\mathrm{Pr}\theta'=0 \tag{18}$$

where K denotes the dimensionless viscosity ratio, defined as follows:

$$K=\frac{\varkappa}{\mu} \tag{19}$$

The boundary conditions (9) and (10) can be rewritten as

$$f=f'=0,\ h=-\frac{1}{2}f'',\ \theta=1 \quad \text{on } \eta=0 \tag{20}$$

$$f'\to 1,\ h\to 0,\ \theta\to 0 \quad \text{as } \eta\to\infty \tag{21}$$

As aforementioned, the gyration is taken to be equal to the angular velocity at the body surface. The solution of micro-inertia density (17) satisfying (20) is

$$i=If^{\frac{2(1-m)}{1+m}} \tag{22}$$

where I is a dimensionless constant.

If the viscosity ratio K is not zero, but I is taken to be zero, from Eq. (16) we find

$$h=-\frac{1}{2}f'' \tag{23}$$

that is, gyration is identical to the angular velocity. Then Eq. (15) becomes

$$\left[1+\frac{K}{2}\right]f'''+ff''+\frac{2m}{m+1}[1-(f')^2]=0 \tag{24}$$

This equation can be reduced to the Blasius equation with a simple changes of dependent variable.

The expression for the shear and couple stresses within the limits of boundary layer theory and in terms of similarity variables are

$$\tau_{yx}=\mu(1+K)\left[\frac{(m+1)U(x)}{2\nu x}\right]^{1/2}\times U(x)\left[f''+\frac{K}{1+K}h\right] \tag{25}$$

$$m_{yz}=\mu\left[1+\frac{K}{2}\right]U(x)If^{\frac{2(1-m)}{1+m}}h' \tag{26}$$

The shear stress at the body surface is given by

$$\tau_w=\left[\mu+\frac{\varkappa}{2}\right]\frac{\partial u}{\partial y}\Big|_{y=0}=\mu\left[1+\frac{1}{2}K\right]U(x)g(x)f''(0) \tag{27}$$

Therefore, the local skin friction coefficient can be written as follows:

$$C_f=\frac{2\tau_w}{\rho U^2}=\left[1+\frac{1}{2}K\right]\frac{\sqrt{2(m+1)}}{\sqrt{\mathrm{Re}_x}}f''(0) \tag{28}$$

where Re_x is the local Reynolds number defined in the usual way.

In addition, the local heat flux may be written by Fourier's law as

$$q_w(x)=-k\frac{\partial T}{\partial y}=-k(T_w-T_\infty)\theta'(0)\times\sqrt{\frac{m+1}{2}}\frac{1}{x}\sqrt{\mathrm{Re}_x} \tag{29}$$

The local heat transfer coefficient and Nusselt number are given by

$$h_t(x)=\frac{q_w(x)}{T_w-T_\infty}=-k\theta'(0)\sqrt{\frac{m+1}{2}}\frac{1}{x}\sqrt{\mathrm{Re}_x} \tag{30}$$

$$Nu_x=\frac{h_t x}{k}=-\theta'(0)\sqrt{\frac{m+1}{2}}\sqrt{\mathrm{Re}_x} \tag{31}$$

3. Results and Discussion

The nonlinear governing differential Eqs. (15), (16) and (18) subject to boundary conditions (20)-(21) are solved numerically using the fourth-order Runge-Kutta numerical procedure for several values of K and m, when $I=1$.

In this study the boundary condition at $\eta\to\infty$ is replaced by identical ones at $\eta_{\max}$ which is a sufficiently large value of η where the velocity

profile f' has approached the free stream velocity to high accuracy. A spanwise step size $\Delta\eta$ of 0.001 is used with $\eta_{max}=8$. In order to verify the accuracy of the present computer simulation model, the results are compared with the accepted data sets for Newtonian fluids over a wedge and the micropolar boundary layer flow over a semi-infinite plate corresponding to the case computed by Ahmadi (1976), and showed a good agreement.

In Figs. 2~8 we have shown some graphs of the characteristic of flow and temperature fields of anisotropic fluids as a function of η. Furthermore, the values, $f''(0)$, $C_f\sqrt{\mathrm{Re}_x}$, $-h(0)$ and Nusselt number with K and m as parameters have been tabulated in Table 1. The numerical values indicate that increasing value of the material parameter K results in a decrease in the values of $f''(0)$ and $-h(0)$. This is because as K increases, the velocity and angular velocity become larger and thus give rise to a reduction in the skin friction and wall couple stress.

Table 1 The effect of variation of K and m on the velocity, skin friction coefficient, gyration field and Nusselt number at the surface for $Pr=1$

β	K	$f''(0)$	$C_f\sqrt{\mathrm{Re}_x}$	$-h(0)$	Nu
	0.00	0.4696	0.3321	0.2348	0.3321
	0.01	0.4679	0.3325	0.2340	0.3309
0°	0.02	0.4661	0.3329	0.2331	0.3296
(m=0.0)	0.03	0.4639	0.3329	0.2320	0.3280
	0.04	0.4602	0.3319	0.2301	0.3254
	0.05	0.4519	0.3275	0.2259	0.3195
	0.00	0.7319	0.5533	0.3660	0.5533
	0.03	0.7209	0.5531	0.3605	0.5450
45°	0.05	0.7110	0.5509	0.3555	0.5375
(m=1/7)	0.08	0.6866	0.5398	0.3433	0.5190
	0.10	0.6523	0.5177	0.3261	0.4931
	0.00	0.9277	0.7574	0.4638	0.7574
	0.05	0.9040	0.7565	0.4520	0.7381
90°	0.10	0.8790	0.7536	0.4395	0.7177
(m=1/3)	0.15	0.8525	0.7483	0.4263	0.6961
	0.20	0.8238	0.7399	0.4119	0.6727
	0.00	1.0904	0.9753	0.5452	0.9753
	0.05	1.0607	0.9724	0.5303	0.9487
135°	0.10	1.0314	0.9686	0.5157	0.9225
(m=3/5)	0.15	1.0024	0.9638	0.5012	0.8966
	0.20	0.9737	0.9580	0.4868	0.8708

The variation of dimensionless velocity f' with η is shown in Fig. 2 for various wedge angles and material parameters. It is difficult to show clearly the corresponding streamwise velocity profiles due to very little variation. The numerical results show that the magnitude of velocity is smaller for

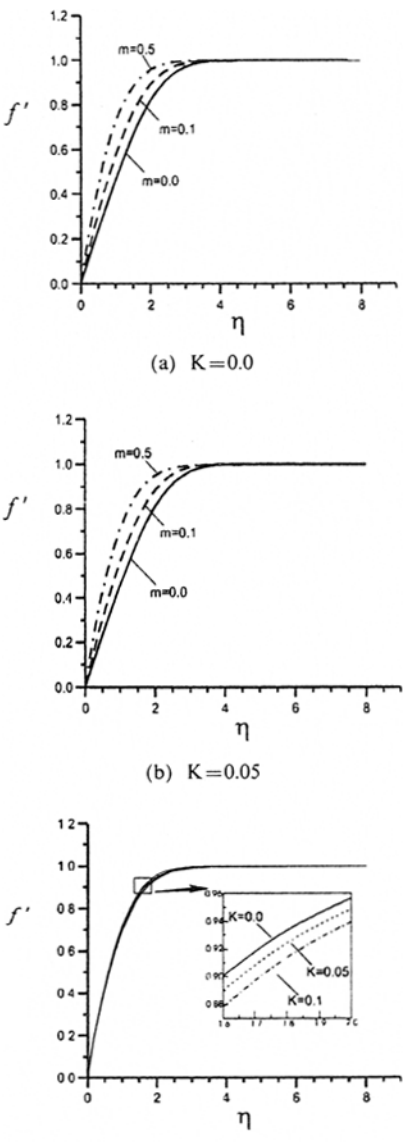

(a) K=0.0

(b) K=0.05

(c) m=0.5

Fig. 2 Distribution of velocity profile f' with η for various K and m with $I=1$

anisotropic fluid with a fixed wedge angle, as compared to Newtonian fluid ($K=0$) when the Falkner-Skan parameter m is constant. For the case of a constant viscosity parameter K, however, where it is seen that for accelerating flows ($m, \beta>0$), the velocity boundary layer is thinner than for a flat plate at zero incidence.

Figure 3 shows the distribution of gyration field h with η for various values of K and m with $I=1$. It is observed that the absolute values of gyration for small wedge angles (less than 90°) first increase to a maximum and then decays to zero. The curves show that the peak value of gyration vector increases rapidly as K increases. Furthermore, the gyration boundary layer thickness is several times greater than that of the

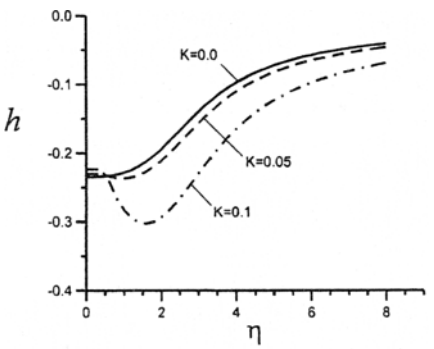

(a) m=0.0

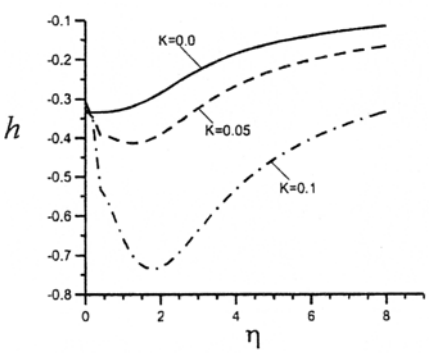

(b) m=0.1

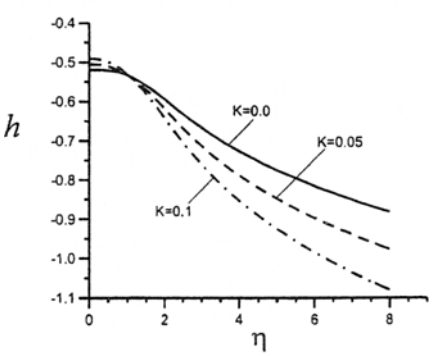

(c) m=0.5

Fig. 3 Distribution of gyration field h with η for various K and m with $I=1$

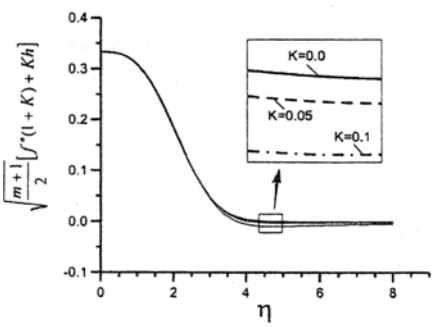

(a) m=0.0

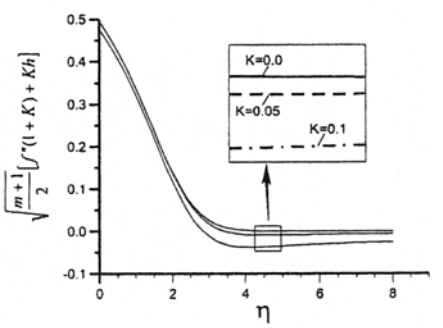

(b) m=0.1

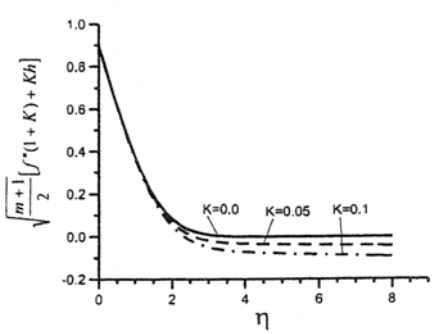

(c) m=0.5

Fig. 4 Distribution of shear stress, $\tau_{yx}/\left[\dfrac{\mu U(x)}{x}\times\sqrt{\mathrm{Re}_x}\right]$, for various K and m with $I=1$

velocity boundary layer, and it also increases with K. However, there is a growing tendency on the absolute values of gyration for the case of $m=0.5$, which denotes the wedge angle 120°.

Figure 4 shows the variation of shear stress, $\tau_{xy}/\left[\frac{\mu U(x)}{x}\sqrt{\mathrm{Re}_x}\right]$, across the boundary layer for different values of K and m. Slight variation of shear stress distribution with K is observed. The results show that the shear stress distribution is lower in the case of the anisotropic fluid case when compared with the Newtonian fluid case while the Falkner-Skan parameter of the problem is held constant.

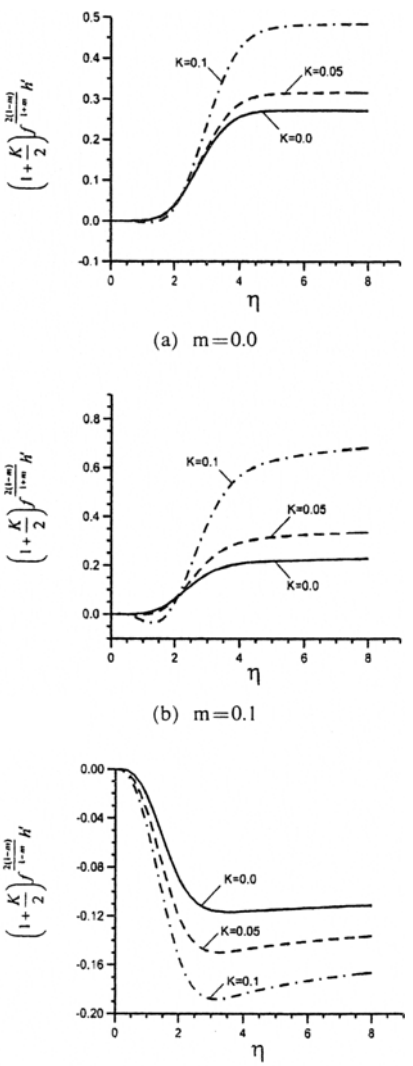

Fig. 5 Distribution of couple stress, $m_{yz}/[\mu U(x) \times I]$, for various K and m with $I=1$

The couple stress, $m_{yz}/[\mu U(x) I]$, distributions across the boundary layer are shown in Fig. 5 for various values of K and m with $I=1$. For the case of a flat plate at zero incidence ($m=0$), the couple stress is zero at the wedge surface. And it becomes slightly negative and then increases and reaches a constant value for each value of K at the edge of the boundary layer, as described in Ahmadi (1976). However, for the case of wedge angle 120°, the couple stresses tend to decrease and then reach a constant value as the distance η from the surface increases. This is because as K increases, the velocity and angular velocity become larger and thus give rise to a reduction in the skin friction and wall couple stress.

Figure 6 shows the distribution of dimensionless temperature profiles for Newtonian fluid ($K=0$) with $Pr=1$ for various wedge angles. The numerical results show that the effect of increasing values of wedge angle, β, results in a decreasing thermal boundary layer thickness and more uniform temperature distribution across the boundary layer.

Figure 7 displays the effects of a dimensionless material parameter K on the dimensionless temperature profiles for various wedge angles with $Pr=1$. These trends show that the thickness of thermal boundary layer is increased with the material parameter K. It is also observed that as β increases for fixed values of Pr and K, the surface heat transfer rate increases due to enhancement of flow velocities.

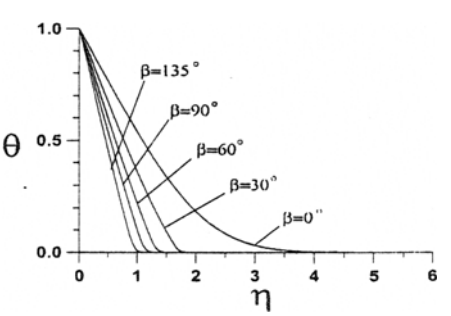

Fig. 6 Effects of wedge angles on the dimensionless temperature profiles for Newtonian fluid ($K=0$) with $Pr=1$

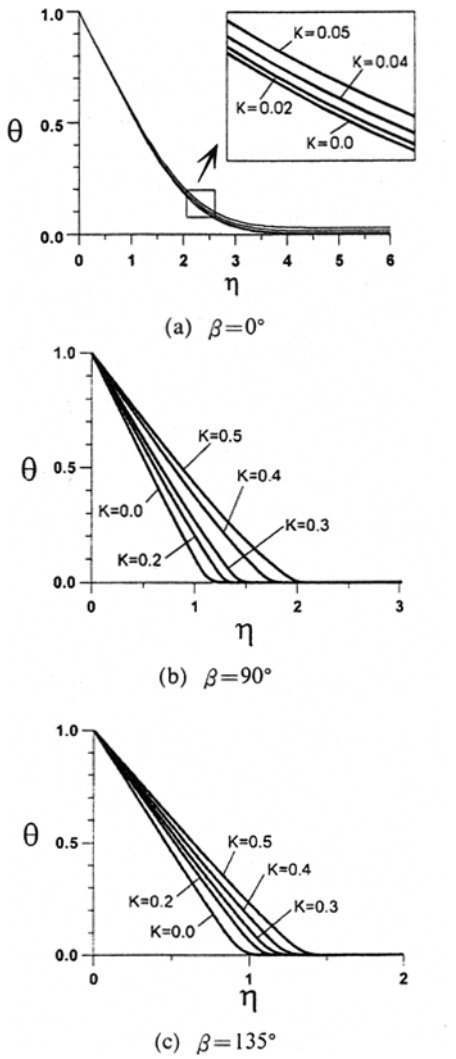

Fig. 7 Effects of material parameter K on the dimensionless temperature profiles for various wedge angles with $Pr=1$

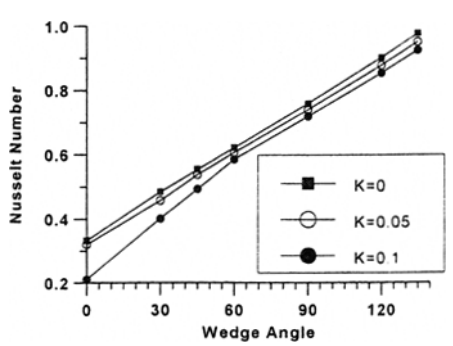

Fig. 8 Nusselt number, $Nu_x/\sqrt{Re_x}$, variations for various wedge angles with $Pr=1$

Figure 8 shows the Nusselt number, $Nu_x/\sqrt{Re_x}$, variations for various wedge angles with $Pr=1$. The results show that the Nusselt number increases linearly with the wedge angle, and slight variation of heat transfer distribution with K is observed. However, the surface heat transfer rate is lower in the case of an anisotropic fluid when compared with the Newtonian fluid while the parameters of the problem are held constant.

4. Concluding Remarks

We have used the theory of micropolar fluids due to Eringen to formulate a set of ordinary differential governing equations for a steady, incompressible, anisotropic fluid in the vicinity of a wedge whose surface is maintained at a constant temperature. The numerical results are presented to illustrate the details of the flow and heat transfer characteristics and their dependence on the material properties of the anisotropic fluid.

It has been shown that the velocity profile changes slightly in the range of the values studied but the gyration and couple stress vary appreciably with small changes in parameters. In addition, the numerical results indicate that, keeping m constant, the skin friction coefficient is lower for anisotropic fluid, as compared with Newtonian fluid.

It has been also observed that for a constant wedge angle with a given Prandtl number, $Pr=1$, the effect of increasing values of K results in an increasing thermal boundary layer thickness for anisotropic fluid, as compared with Newtonian fluid. For the case of the constant material parameter K, however, the heat transfer rate for anisotropic fluid is lower than that of Newtonian fluid. The accuracy of the present study cannot be assessed at this time because of the lack of experimental data.

References

Ahmadi, G., 1976, "Self-Similar Solution of Incompressible Micropolar Boundary Layer Flow over a Semi-Infinite Plate," *Int. J. Engng*

Sci., Vol. 14, pp. 639~646.

Ariman, T., 1971, "On the Analysis of Blood Flow," *J. Biomech.*, Vol. 4, pp. 185~192.

Bergholz, R. F., 1980, "Natural Convection of a Heat Generating Fluid in a Closed Cavity," *J. Heat Transfer*, Vol. 102, pp. 242~247.

Shekar, C. B., Vasseur, P., Robillard, L. and Nguyen, T. H., 1984, "Natural Convection in a Heat Generating Fluid Bounded by Two Horizontal Concentric Cylinders," *Can. J. Chem. Engng.*, Vol. 62, pp. 482~489.

Emara, A. A. and Kulacki, F. A., 1980, "A Numerical Investigation of Thermal Convection in a Heat-Generating Fluid Layer," *J. Heat Transfer*, Vol. 102, pp. 531~537.

Eringen, A. C., 1966, "Theory of Micropolar Fluids," *J. Math. Mech.*, Vol. 16, pp. 1~18.

Eringen, A. C., 1972, "Theory of Thermomicrofluids," *J. Math. Analysis Applic.*, Vol. 38, pp. 480~496.

Falkner, A. C. and Skan, S. W., 1931, "Some Approximate Solutions of the Boundary Layer Equations," *Phil. Mag.*, Vol. 12, No. 7, pp. 865~896.

Gorla, R. S. R., 1980, "Thermal Boundary Layer of a Micropolar Fluid at a Stagnation Point," *Int. J. Engng Sci.*, Vol. 18, pp. 611~617.

Gorla, R. S. R., 1984, "The Axisymmetric Micropolar Boundary Layer on a Long Thin Cylinder," *Int. J. Engng Sci.*, Vol. 22, pp. 293~299.

Gorla, R. S. R., 1985, "Axisymmetric Thermal Boundary Layer of a Micropolar Fluid on a Cylinder," *Int. J. Engng Sci.*, Vol. 23, pp. 401~407.

Rees, D. A. S. and Bassom, A. P., 1996, "The Blasius Boundary-Layer Flow of a Micropolar Fluid," *Int. J. Engng Sci.*, Vol. 34, No. 1, pp. 113~124.

Willson, A. J., 1970, "Boundary Layers in Micropolar Liquids," *Proc. Camb. Philol. Soc.*, Vol. 67, pp. 469~476.